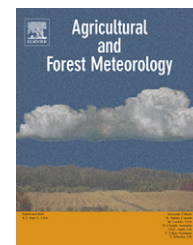


available at www.sciencedirect.comjournal homepage: www.elsevier.com/locate/agrformet

An improved estimate of leaf area index based on the histogram analysis of hemispherical photographs

Robinson I. Negrón Juárez^{a,*}, Humberto Ribeiro da Rocha^a,
Adelaine Michela Silva e Figueira^b, Michael L. Goulden^c, Scott D. Miller^d

^a Department of Atmospheric Sciences, University of São Paulo, São Paulo, SP, Brazil

^b CENA, University of São Paulo, SP, Brazil

^c Department of Earth System Science, University of California, Irvine, CA, USA

^d Atmospheric Sciences Research Center, State University of New York, NY, USA

ARTICLE INFO

Article history:

Received 17 August 2007

Received in revised form

16 April 2008

Accepted 11 November 2008

Keywords:

Hemispherical photography

Histogram

Optimal threshold value

Gap fraction

Litterfall

Leaf area index (LAI)

ABSTRACT

Leaf area index (LAI) is a key parameter that affects the surface fluxes of energy, mass, and momentum over vegetated lands, but observational measurements are scarce, especially in remote areas with complex canopy structure. In this paper we present an indirect method to calculate the LAI based on the analyses of histograms of hemispherical photographs. The optimal threshold value (OTV), the gray-level required to separate the background (sky) and the foreground (leaves), was analytically calculated using the entropy crossover method (Sahoo, P.K., Slaaf, D.W., Albert, T.A., 1997. Threshold selection using a minimal histogram entropy difference. *Optical Engineering* 36(7) 1976–1981). The OTV was used to calculate the LAI using the well-known gap fraction method. This methodology was tested in two different ecosystems, including Amazon forest and pasturelands in Brazil. In general, the error between observed and calculated LAI was ~6%. The methodology presented is suitable for the calculation of LAI since it is responsive to sky conditions, automatic, easy to implement, faster than commercially available software, and requires less data storage.

© 2008 Elsevier B.V. All rights reserved.

1. Introduction

Leaf area index (LAI), defined as the one-sided green leaf area per unit ground area (m^2/m^2) is an important parameter in climate studies and is a key parameter used in land surface parameterizations. Leaf area determines substantially the vegetation–atmosphere exchanges of energy, momentum and mass (Monteith and Unsworth, 1990; Myneni et al., 2007). A reduction in LAI decreases transpiration (Parton et al., 1996), affecting the biochemical and hydrological cycle. Therefore, accurate representation of the seasonality and spatial varia-

bility of LAI should improve estimates of surface water balance and productivity (Wright et al., 1996; Huete et al., 2006), and consequently improve estimates of both deforestation and global warming impacts on regional and global climate (Nobre et al., 2004; Costa and Foley, 2000). Direct measurements of LAI are laborious, destructive, and may not represent well the large spatial variability of complex canopy structure (Roberts et al., 1996). The gap fraction method, an indirect approach, has been widely used to estimate LAI (Norman and Campbell, 1989) through the use of below-canopy hemispherical images. The Norman and Campbell

* Corresponding author. Current address: Ecology and Evolutionary Biology, Tulane University, 6823 St. Charles Ave., Rm# 400 Boggs Center, New Orleans, LA 70118-5698, USA. Tel.: +1 504 862 8285.

E-mail addresses: rjuarez@tulane.edu (R.I. Negrón Juárez), humberto@iag.usp.br (H.R. da Rocha), michela@cena.usp.br (A.M.S. e Figueira), mgoulden@uci.edu (M.L. Goulden), smiller@albany.edu (S.D. Miller).

0168-1923/\$ – see front matter © 2008 Elsevier B.V. All rights reserved.

doi:10.1016/j.agrformet.2008.11.012

method assumes that the distribution of foliage elements is randomly dispersed, therefore the LAI for clumped canopy may be underestimated (van Gardingen et al., 1999; Stenberg, 1996).

The advantages of using hemispherical images including high-resolution images to estimated LAI are discussed in Jonckheere et al. (2004) and Weiss et al. (2004). Its analysis requires the identification of two classes: the target or foreground (the leaves), and the background (the sky). This separation implies that the classes have distinct intensities, that is, thresholding the set of gray-levels into the background and the target by using the gray-scale histogram of an image (Sahoo et al., 1988; Jansing et al., 1999). Jonckheere et al. (2005) presents a comparison of different threshold method for hemispherical photographs. Uncertainties in LAI from commercially available software to process hemispherical photographs are expected since the threshold selection is performed arbitrarily. Other errors depend on the field sampling strategy, including variation of zenith angle, diffuse fraction, and the intensity of solar radiation. The objective of this paper is to introduce an improved threshold selection method based on histogram analysis to calculate LAI. The proposed methodology was validated by comparing observed LAI over two contrasting vegetation types including the Amazon rainforest and pasture.

2. Material and methods

2.1. Sites

Hemispherical photographs and observed data were collected in two experimental sites, a tropical forest and a pastureland site in eastern Amazonia. The Amazon forest site is located in the Tapajos National Forest, near a 67 m micrometeorological tower (3°1'1.2"S; 54°58'14.5"W) installed near the km 83 post of BR-163 (Cuiabá-Santarém highway), 70 km south of Santarém, Pará, Brazil, and at 153 m above sea level (Goulden et al., 2004). The vegetation is dense tropical humid forest with a canopy height of ~35–40 m, with yellow dystrophic latosol (clay oxisol) soil. The annual mean precipitation and temperature is 1911 mm and 25 °C, respectively, with the dry season defined from July to November. Evapotranspiration ranges between ~4 mm day⁻¹ in the dry season and ~3 mm day⁻¹ in the wet season (da Rocha et al., 2004). Dominant tree species include the tauari (*Couratari guianensis*), matamatá (*Eschweilera* sp.), maçaranduba (*Manilkara huberi*), andiroba (*Carapa guianensis*), tachi (*Sclerolobium paniculatum*), abiu (*Pouteria* sp.), breu (*Protium decandro*), and louro (*Licaria Guianensis*) (Sousa et al., 2003). The site was selectively logged in September 2001, removing 12% of the canopy at our measurement site (Miller et al., 2007).

The pastureland site is located in Santarém, Pará state, Brazil, near a 20 m micrometeorological tower (3°0.714'S; 54°32'11.47"W) installed at ~5 km east of the km 77 post of the BR-163 Highway. Following deforestation in 1991, the site was a cattle ranch covered with managed grass (*Brachiaria Brizantha*) (Sakai et al., 2003). The altitude, climate and soil patterns are similar to those of the forest site. In November 2001, the site was burned, plowed, and converted to a rice plantation.

2.2. Data

Hemispherical photographs (hereafter simply referred to as images) were collected using the CI-110 Digital Plant Canopy Imager (CID Inc., Camas, WA, USA) mounted on a tripod, aligned to magnetic north, leveled to 90 cm height above-ground (to the soil surface in the pastureland), and connected to a notebook computer. The device deploys a 150° fish-eye lens image, recorded as 180,912 pixels, 24-bits gray-level files (BMP format) with 3 × m × n arrays. The set of images were captured using an azimuth angle range from 0° to 360°, and its zenith angle from 0° to 75°. The image files were converted into eight-bit (2D) images by extracting one channel, which reduced to one-third the storage size. This procedure is justifiable since at the gray-level the three channels (blue, red, yellow) have the same values. The histogram analysis was performed using the converted set of images. For the analysis, each image was divided into seven 10°-strips from 5° to 75° and the gap fraction and LAI were calculated for each annulus in a pixel-per-pixel basis (using the Interactive Data Language – IDL – 6.0 running on a 1 GHz pentium III pc machine). LAI was also calculated using the device software (CI-110, Production 1.0, CID Inc. 1997, 1998, hereafter referred to as CI-LAI). During image capture, the brightness (luminosity) and contrast (between background and foreground) were tuned to provide visual quality. In general it was observed that high and low brightness values often led to low and high estimates of LAI, respectively. Although contrast and brightness should combine to give better estimates of LAI, their tuning also depended on sky luminosity and canopy architecture.

At the forest site, images were collected at nodes of a 300 m × 600 m regular grid that extended 500 m east, 100 m west, 150 m south, and 150 m north of the flux tower (Fig. 1). Litterfall was collected from September 2000 to August 2002 on a bi-weekly basis, over thirty 1 m²-traps 25 m intervals along two east-west transects (rows I and E, full circles in Fig. 1) (see Goulden et al., 2004 for details). The LAI estimated from litterfall collection will be denoted as litter-LAI. In the pasture site, six images were collected at each of three 1 m²-plots (referred to as A, B, C) on 6 June 2001, during overcast sky condition. At this site, the observed LAI was obtained by the destructive method immediately after image collection.

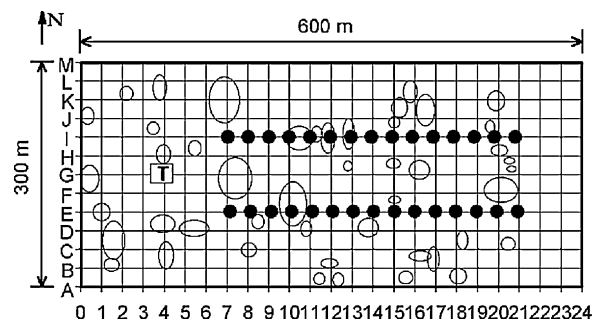


Fig. 1 – Regular grid used under the tropical forest site to collect litterfall and below-canopy hemispheric images. Full circles are litterfall traps, ellipses are the gaps created by the selective logging (after September 2001), and T is the micrometeorological tower (3°1'1.2"S, 54°58'14.52"W).

2.3. Calculated LAI using the entropy crossover method

We describe briefly the entropy crossover method (ECOM) for calculating the optimal threshold value (OTV) to separate the two classes of images (Sahoo et al., 1988, 1997). The *a priori* entropy of the image, *E*, is

$$E = - \sum_{i=100}^{255} p_i \log_2 p_i \tag{1}$$

where p_i is the density function or the normalized histogram (number of pixels with gray-level i , upon the total number of pixels). Let BP and WP be classes of black and white pixels, respectively. The *a priori* entropies for BP, E_{BP} , and for WP, E_{WP} , are defined using the threshold value, t , as

$$E_{BP} = - \sum_{i=100}^t \left(\frac{p_i}{p(BP)} \log_2 \frac{p_i}{p(BP)} \right) \tag{2}$$

$$E_{WP} = - \sum_{i=t+1}^{255} \left(\frac{p_i}{p(WP)} \log_2 \frac{p_i}{p(WP)} \right)$$

where $p(BP) = \sum_{i=100}^t p_i$, $p(WP) = \sum_{i=t+1}^{255} p_i$, and $p(BP) + p(WP) = 1$. The OTV is calculated by finding the gray-level where the entropy functions E_{BP} and E_{WP} are equal, con-

strained by $(E_{BP} - E_{WP})^2$ is minimum, $\forall t \in (100, 255)$, so that the two functions crossover the gray-level dependence. The assumption that the OTV is in the range of 100-255 was determined from an initial histogram analysis and its main benefit is the reduction of the time processing. Examples of images collected are shown in Fig. 2(a and b), and the processed thresholded images with OTV are shown in Fig. 2(c and d). In this example the OTVs were 183 and 130 for forest and pasture, respectively.

To calculate the LAI we use the gap fraction method described in Norman and Campbell (1989). Briefly, the transmitted fraction (T) of a beam of radiation in a canopy with randomly distributed elements is given by the Beer-Lambert equation as

$$T(z_i) = \exp \left(- \frac{K_{ij}(z_i, \alpha) \times PAI}{\cos(z_i)} \right) \tag{3}$$

where K_{ij} is the extinction coefficient at a zenith angle z_i for a class of leaves j with inclination angle α . PAI is the effective plant area index. The extinction coefficient can be defined using a generalized ellipsoidal leaf angle distribution model proposed by Campbell (1986)

$$K_i = \frac{\sqrt{x^2 + \tan^2 \theta_i}}{x + 1.774(x + 1.182)^{-0.733}} \tag{4}$$

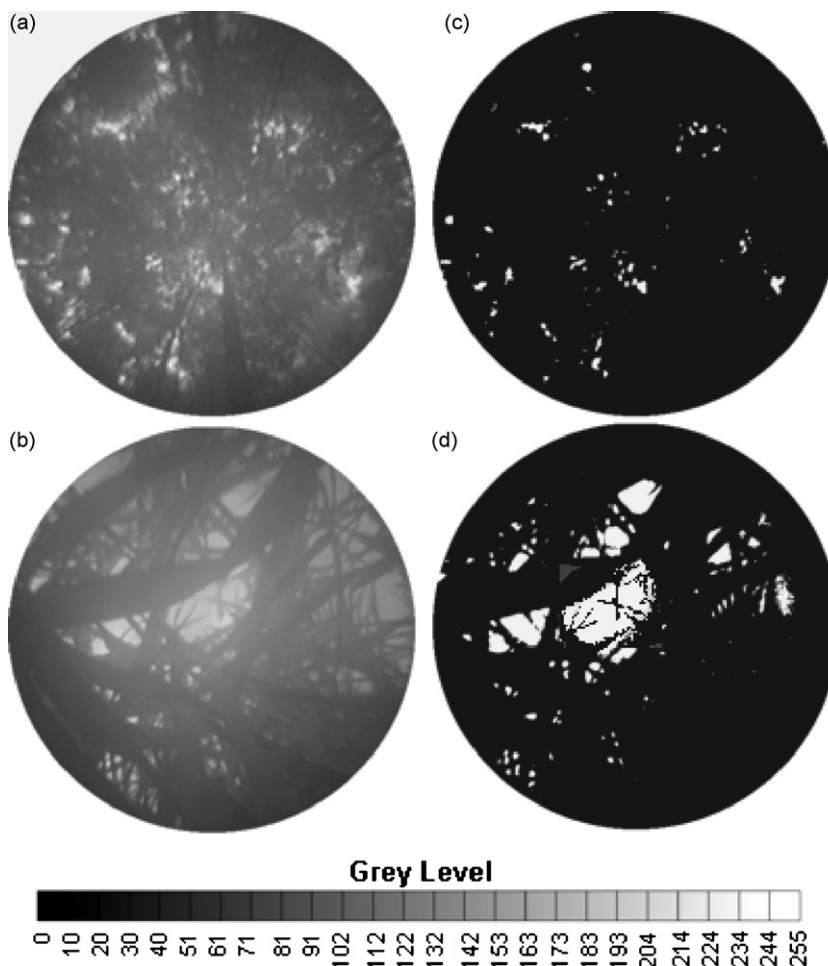


Fig. 2 – Below-canopy hemispherical photographs in the tropical forest (a, c), and Pastureland (b, d). Images (a, b) collected with the CI-110 device, and images (c, d) were thresholded by optimal threshold values equal to 183 and 130, respectively.

Therefore a single parameter, x , determines the shape of the distribution. Eq. (3) can be solved for PAI and x using nonlinear least-squares regression technique. PAI is expressed as

$$PAI = C \times LAI + WAI \tag{5}$$

where LAI is the leaf area index, WAI is the wood area index that depends on the vegetation type, and C is the clumping factor (Nilson, 1971). A more accurate formulation for PAI should include a clumping factor for WAI. LAI was calculated in (5) using prescribed C and WAI (hereafter referred to as ECOM-LAI).

The mean square error (MSE) between the transmitted light fraction optimized by the bisection method ($T_{\text{predicted}}$), and the transmitted light fraction measured over the seven annulus (T_{measured}) is defined as

$$MSE = \left[\frac{1}{7} \sum_1^7 (T_{\text{Predicted}} - T_{\text{Measured}})^2 \right]^{1/2} \tag{6}$$

The nonlinear least-square regression searches for values of x that will produce a reasonable fit to the input data of $T(z_i)$. If the input data is inconsistent or contains too much error, large values of x are needed to avoid negative values of LAI (Norman and Campbell, 1989). We observed that large constraints of x produced not only MSE larger than 1 but also discontinuities in the LAI vs. gray-level curve. Since LAI is less sensitive to error than x (Norman and Campbell, 1989) we used the MSE as a simple metric to accept or reject calculated LAI based on the following criteria: LAI is accepted if $0 \leq MSE < 1$; LAI is rejected if $MSE \geq 1$. For simplicity, the MSE values larger than 1 were

truncated to 1. The IDL software which performs the LAI calculation following the procedure described above is available at ftp://lba.cptec.inpe.br/lba_archives/CD/CD-04/lai/gap_fraction/. On average the time required to process 100 images was 15 min.

3. Results and discussions

3.1. Tropical rainforest

Samples of calculated PAI, MSE, E_{BP} , E_{WP} , and the histogram for two images at the forest site collected during overcast sky condition are shown in Fig. 3(a and b). The histograms show a high frequency around the gray-level 100, and then decrease with the smallest frequencies at gray-level 190. The peak at the gray-level 255 corresponds to the brightest pixels in the image. The transition zone from the foreground to background was expected to appear as an abrupt change in the histogram. However, this was not observed, likely because of the penumbra effect as a blurring zone between the leaves and the sky, but possibly also due to leaf reflection, leaf movement by wind and even pixel-size resolution (not specified by the manufacturer). The calculated OTV for these two images was 182 and 183 with a PAI value of 7 and $5 \text{ m}^2 \text{ m}^{-2}$, respectively. PAI in Fig. 3(b) had to be rejected because the MSE between measured and predicted transmitted light fraction at the calculated OTV was greater than 1.

Assuming that leaves recycle in 1 year, the accumulated literfall collected in row I and E (data available at ftp://lba.cptec.inpe.br/lba_archives/CD/CD-04/lai) during Septem-

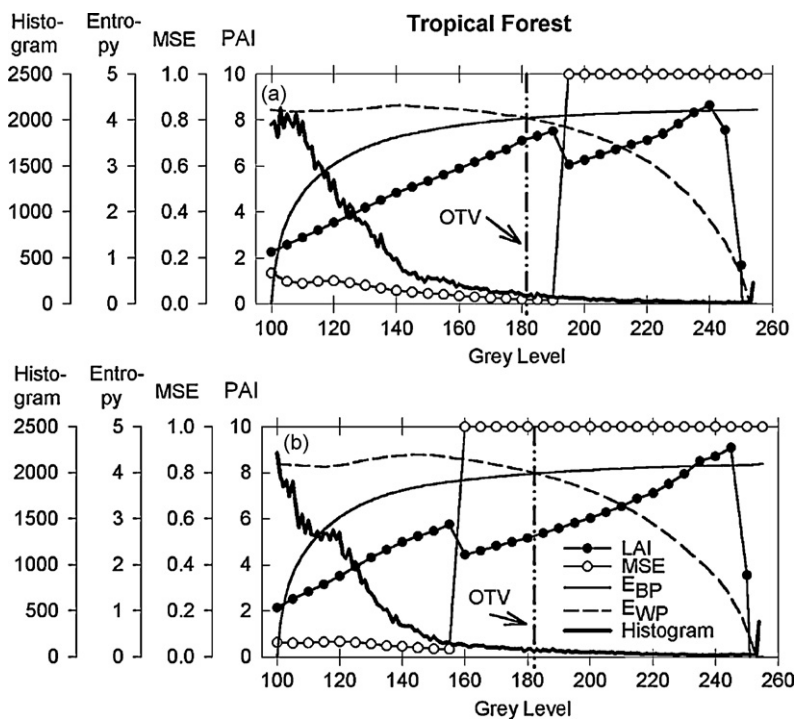


Fig. 3 – Calculated PAI (full circles), MSE (open circles), E_{BP} (solid line), E_{WP} (dash line), and histogram (thick solid line) as number of gray-level elements for two hemispherical photographs (a: grid point M1 and b: grid point M4) taken in overcast sky conditions during the early morning on 1 June 2001, in the tropical forest site. Vertical dash-dot-dot line intercepts the crossover point (between the entropies E_{BP} and E_{WP}) and the optimal threshold value (OTV).

Table 1 – Calculated effective plant area index (PAI) and leaf area index (LAI) before and after logging over a 300 m × 600 m block (325 points of a regularly spaced grid; see Fig. 3(a)) using hemispherical photograph (HPs). Monthly average values are also shown. The site is located in the Amazon forest at FLONA Tapajos, Santarén (km 83), Pará, Brazil.

| Year | Month | Row | Number of HPs used | PAI | LAI | Average LAI | | |
|--------------------|----------|----------|--------------------|------|-------------|-------------|-------------|------|
| <i>Undisturbed</i> | | | | | | | | |
| 2000 | June | A | 05 | 4.90 | 6.36 | 5.70 ± 0.28 | | |
| | | B | 16 | 4.03 | 5.23 | | | |
| | | C | 29 | 4.60 | 5.97 | | | |
| | | D | 34 | 4.36 | 5.66 | | | |
| | | E | 31 | 4.40 | 5.71 | | | |
| | | F | 35 | 4.26 | 5.53 | | | |
| | | G | 33 | 4.25 | 5.52 | | | |
| | | H | 34 | 4.18 | 5.43 | | | |
| | | I | 30 | 4.34 | 5.64 | | | |
| | | J | 29 | 4.51 | 5.86 | | | |
| | | K | 28 | 4.39 | 5.70 | | | |
| | | L | 23 | 4.51 | 5.86 | | | |
| | | M | 23 | 4.28 | 5.56 | | | |
| 2001 | May | C | 05 | 5.17 | 6.71 | 6.13 ± 0.45 | | |
| | | E | 12 | 4.64 | 6.03 | | | |
| | | G | 10 | 4.99 | 6.48 | | | |
| | | H | 04 | 4.66 | 6.05 | | | |
| | | I | 13 | 4.15 | 5.39 | | | |
| | | M | 12 | 4.73 | 6.14 | | | |
| | July | I | 13 | 3.93 | 5.10 | 5.21 ± 0.16 | | |
| | | E | 12 | 4.10 | 5.32 | | | |
| | December | A | 13 | 3.05 | 3.96 | 4.26 ± 0.46 | | |
| | | E | 11 | 2.95 | 3.83 | | | |
| | | G | 14 | 3.74 | 4.86 | | | |
| | 2002 | February | I | 11 | 3.59 | 4.66 | 4.69 ± 0.78 | |
| | | | H | 02 | 3.08 | 4.00 | | |
| B | | | 03 | 3.26 | 4.23 | | | |
| C | | | 02 | 4.03 | 5.23 | | | |
| D | | | 02 | 2.44 | 3.17 | | | |
| E | | | 08 | 3.17 | 4.12 | | | |
| F | | | 03 | 4.22 | 5.48 | | | |
| G | | | 15 | 3.31 | 4.30 | | | |
| H | | | 02 | 3.63 | 4.71 | | | |
| I | | | 10 | 4.01 | 5.21 | | | |
| J | | | 01 | 3.74 | 4.86 | | | |
| K | | | 01 | 2.93 | 3.81 | | | |
| L | | | 02 | 4.19 | 5.44 | | | |
| M | 01 | 4.43 | 5.75 | | | | | |
| March | E | 06 | 2.85 | 3.70 | 3.91 ± 0.29 | | | |
| | I | 13 | 3.17 | 4.12 | | | | |
| April | F | 4 | 3.78 | 4.91 | 5.05 ± 0.19 | | | |
| | G | 3 | 3.99 | 5.18 | | | | |
| May | A | 2 | 3.97 | 5.16 | 4.80 ± 0.56 | | | |
| | C | 2 | 4.44 | 5.77 | | | | |
| | D | 2 | 4.09 | 5.31 | | | | |
| | E | 3 | 3.61 | 4.69 | | | | |
| | F | 2 | 3.28 | 4.26 | | | | |
| | G | 3 | 3.51 | 4.56 | | | | |
| | H | 4 | 2.97 | 3.86 | | | | |
| | J | 3 | 3.71 | 4.82 | | | | |
| | K | 4 | 3.25 | 4.22 | | | | |
| | L | 3 | 3.70 | 4.81 | | | | |
| | M | 3 | 4.09 | 5.31 | | | | |
| October | E | 14 | 3.03 | 3.94 | 3.89 ± 0.06 | | | |
| | I | 13 | 2.96 | 3.84 | | | | |
| <i>Logged</i> | | | | | | | | |
| 2003 | February | I | 14 | 3.21 | 4.17 | 4.17 | | |
| | | March | E | 9 | 3.23 | | 4.19 | |
| | | | I | 7 | 3.34 | | 4.34 | |
| | April | E | 14 | 3.09 | 4.01 | 4.12 ± 0.15 | | |
| | | I | 12 | 3.25 | 4.22 | | | |
| | May | E | 13 | 3.07 | 3.99 | 4.36 ± 0.41 | | |
| | | I | 14 | 3.41 | 4.43 | | | |
| | | G | 11 | 3.26 | 4.23 | | | |
| | | L | 7 | 3.18 | 4.13 | | | |
| | | M | | | 4 | | 3.87 | 5.03 |

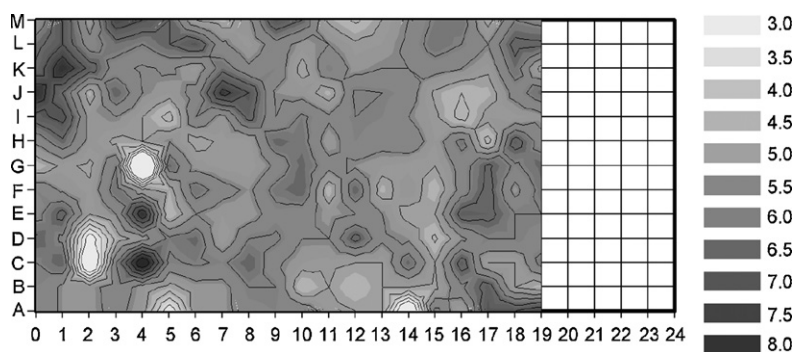


Fig. 4 – Spatial distribution of calculated ECOM-LAI ($\text{m}^2 \text{m}^{-2}$) over the regular grid (see Fig. 1) in the tropical forest based on images collected during 22–23 June 2000.

ber 2000 to August 2001 showed a litter-LAI equals to $5.45 \text{ m}^2 \text{m}^{-2}$, which is comparable to the values between 4.5 and $5.5 \text{ m}^2 \text{m}^{-2}$ reported by Roberts et al. (1996) over central Amazonia using the same methodology. We used the set of images collected during overcast sky condition on 22 and 23 June and 2000 (Table 1) to calculate the ECOM-LAI over the whole grid. Since canopy at this site is very closed we assume $\text{WAI} = 0$. Thus, the mean PAI was calculated to be $4.38 \text{ m}^2 \text{m}^{-2}$ and consequently the clumping factor $C (= \text{PAI}/\text{LAI})$ was 0.8. Using this clumping factor we estimate that the spatial ECOM-LAI over our grid varied from 3 to $8 \text{ m}^2 \text{m}^{-2}$ (Fig. 4) with a mean value was $5.70 \pm 0.23 \text{ m}^2 \text{m}^{-2}$ (Table 1), 5% higher than the litter-LAI. The lowest values observed in Fig. 4 were due to patches with small clearings created during the tower building and a hut. Our result suggests a high spatial variability of LAI over Amazon forest in agreement with other studies. Using vertical radiation measurements over a rainforest in Venezuela, Anhuf and Rollenbeck (2001) found that LAI varied between 1.4 and $6.0 \text{ m}^2 \text{m}^{-2}$, with a mean of $4.24 \text{ m}^2 \text{m}^{-2}$.

We compared the ECOM-LAI and CI-LAI values, using arbitrarily chosen thresholds of 50% (gray-level 127) and 75% (gray-level 191) in the CI-110 software. The LAI obtained were similar: $4.10 \pm 0.62 \text{ m}^2 \text{m}^{-2}$ and $4.20 \pm 0.66 \text{ m}^2 \text{m}^{-2}$, respectively. On average, the CI-LAI underestimated the ECOM-LAI by about 28% and the litter-LAI by 24%. The calculated frequency distributions showed that CI-LAI was systematically lower than ECOM-LAI, with the main mode LAI values from 4 to $4.5 \text{ m}^2 \text{m}^{-2}$, while the ECOM-LAI's main mode showed values from 5.5 to $6 \text{ m}^2 \text{m}^{-2}$ (Fig. 5).

For measurements after logging, the clumping factor had to be reassessed. The LAI from accumulated litterfall from September 2001 to August 2002 was equal to $4.65 \text{ m}^2 \text{m}^{-2}$ that, combined with the calculated ECOM-PAI for May 2002 (equal to $3.69 \text{ m}^2 \text{m}^{-2}$), produced a clumping factor C of 0.79. With this clumping factor, the seasonal ECOM-LAI after logging was $4.40 \pm 0.36 \text{ m}^2 \text{m}^{-2}$ during the wet season (December 2001, February–May 2002, February–May 2003, in Table 1), and $3.89 \pm 0.06 \text{ m}^2 \text{m}^{-2}$ at the end of the dry season (October 2002, Table 1). The average value was $4.52 \text{ m}^2 \text{m}^{-2}$ (~3% lower than observed). The change of ECOM-LAI was of 19.8% before ($5.67 \text{ m}^2 \text{m}^{-2}$) and after the logging ($4.52 \text{ m}^2 \text{m}^{-2}$).

Fig. 6 shows the monthly calculated ECOM-LAI and litterfall rates during the entire data period. The collected litterfall

during 2000, 2001 and 2002 showed a bimodal annual pattern, with maximums in July (late wet to early dry season) and December (late dry season). Before logging and during end of the wet season and early dry season (May–July) the LAI showed maximum values. The persistence of maximum values during this period in different years is consistent with seasonality in LAI as reported by Myneni et al. (2007). Although after-logging data for the same period was not collected, patterns in leaf senescence, with changes in LAI anticipating seasonal changes in precipitation are expected (Goulden et al., 2004). Our results show that ECOM-LAI varied roughly between 4 and $6 \text{ m}^2 \text{m}^{-2}$ with the peak value preceding the maximum litterfall data. The decrease of LAI 1 year after the selective logging has been discussed by Asner et al. (2006) and Miller et al. (2007).

Clumping factor is an important parameter for the calculation of LAI and diverse methods have been proposed for its estimation (Lang and Xiang, 1986; Chen and Black, 1992; Chen and Cihlar, 1995; van Gardingen et al., 1999; Leblanc et al., 2005). Improvements in LAI calculation can be obtained from proper clumping values that vary spatial and temporally. van Gardingen et al. (1999) reported that clumping factor in forests vary between sample and location due to the effect of tree spacing and canopy gaps. Seasonal variation in clumping factor is expected due to senescence and leaf flushing as inferred from litterfall data reported in this study. Improvements in LAI calculation can also be expected from the use of

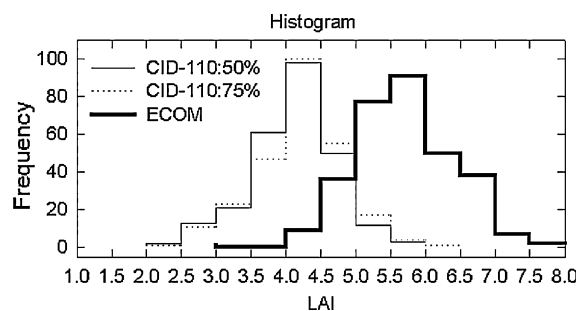


Fig. 5 – Frequency distribution of calculated LAI using ECOM (thick solid line). LAI calculated by CID-110 software at thresholds of 50% (solid line) and 75% (dotted line) are also shown.

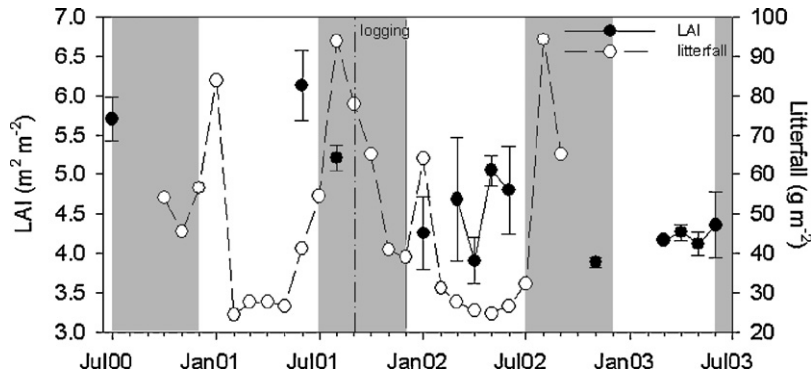


Fig. 6 – Average monthly ECOM-LAI ($\text{m}^2 \text{m}^{-2}$) (full symbol) over the tropical forest site and monthly litterfall ($\text{g m}^{-2} \text{month}^{-1}$) (open symbol) for the period 2000–2003. The dry season is represented by shaded areas and the logging event by the dash-dot line in September 2001.

high-resolution digital images produced by devices currently available and at affordable prices (Jonckheere et al., 2004).

3.2. Pastureland

The histograms, PAI, MSE, E_{BP} , E_{WP} , for two images in the pasture site are shown in Fig. 7. In pasturelands the optical path is shorter than in forest, and consequently the transition zone was well defined (e.g. in Fig. 7(b)). At high luminosity the histogram reached values up to gray-level 240, with a well-

distributed pattern (plot A in Table 2, Fig. 7(a)), whereas during cloudy conditions (dark clouds previous to rainfall) the maximum gray-levels were close to 170 (plot C in Table 2, Fig. 7(b)). Assuming WAI = 0 and the clumping factor equal to 1, the ECOM-LAI in plots A, B, and C were respectively 2.26 ± 0.46 , 2.29 ± 0.93 , and 3.22 ± 0.68 (in $\text{m}^2 \text{m}^{-2}$), with the C.V. varying from 20% to 41% (Table 2), suggesting considerable plant cover variability over each plot, and from plot to plot. The measured LAIs with the destructive method were 2.14, 2.29, and $3.14 \text{ m}^2 \text{m}^{-2}$, for plots A, B, and C, respectively

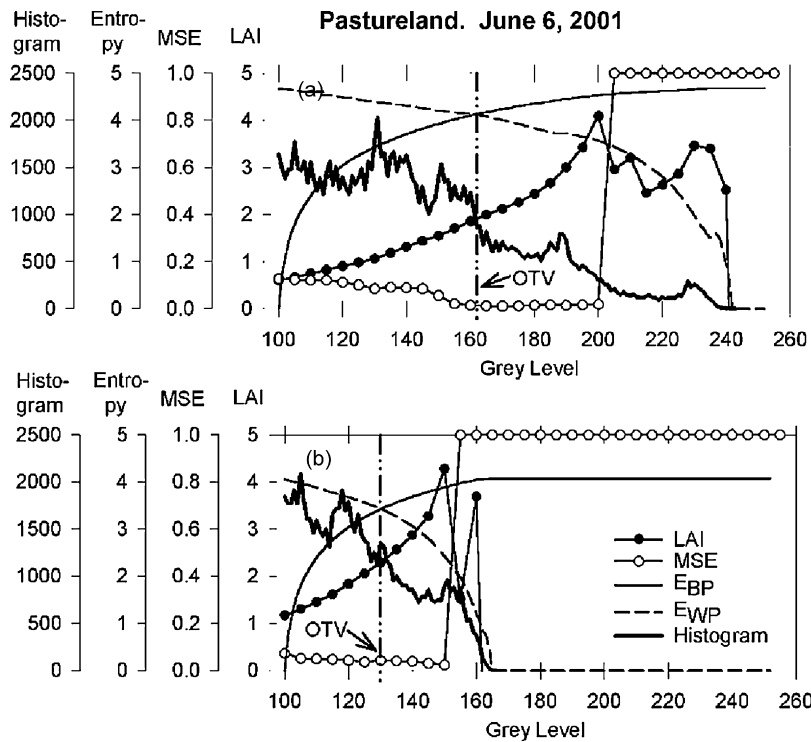


Fig. 7 – Calculated PAI (full circles), MSE (open circles), E_{BP} (solid line), E_{WP} (dash line), and histogram (thick solid line) as number of gray-level elements with dark overcast sky (a) and clear overcast sky (b) on 6 June 2001 at the pasture site. Vertical dash-dot-dot line intercepts the crossover point (between the entropies E_{BP} and E_{WP}) and the optimal threshold value (OTV).

Table 2 – Calculated LAI for each of six hemispherical photographs (HPH) in three 1 m² plots A, B, C, respectively, over pasture land using the entropy crossover method (ECOM-LAI) and the CI-110 software (CI-LAI) at thresholds of 50% and 75%. Measured LAI values obtained from destructive method at each plot are also shown. The difference between measured and calculated values is calculated as: $\text{difference (\%)} = ((\text{LAI}_{\text{calculated}} - \text{LAI}_{\text{measured}}) / \text{LAI}_{\text{measured}}) \times 100$. The site is located in Santarém (km 77), Pará, Brazil. Measurements were collected on 6 June 2001.

| Image | Plot A | | | Plot B | | | Plot C | | |
|------------------------|-------------|-------------|-------------|-------------|-------------|-------------|-------------|-------------|-------------|
| | ECOM-LAI | CI-LAI 50% | CI-LAI 75% | ECOM-LAI | CI-LAI 50% | CI-LAI 75% | ECOM-LAI | CI-LAI 50% | CI-LAI 75% |
| 1st | 2.40 | 0.98 | 1.70 | 1.10 | 1.75 | 2.47 | 2.43 | 1.35 | 2.20 |
| 2nd | 1.53 | 1.37 | 2.24 | 1.77 | 1.54 | 2.38 | 3.48 | 1.91 | 2.79 |
| 3rd | 2.62 | 1.44 | 2.36 | 1.81 | 0.98 | 1.74 | 3.79 | 1.92 | 2.85 |
| 4th | 2.45 | 1.50 | 2.37 | 3.24 | 1.60 | 2.25 | 3.70 | 1.99 | 2.96 |
| 5th | 2.69 | 1.86 | 2.58 | 2.32 | 2.03 | 2.88 | 3.66 | 1.08 | 1.52 |
| 6th | 1.88 | 1.66 | 2.38 | 3.52 | 1.23 | 2.22 | 2.26 | 2.31 | 2.87 |
| Average calculated LAI | 2.26 ± 0.46 | 1.47 ± 0.30 | 2.27 ± 0.30 | 2.29 ± 0.93 | 1.52 ± 0.37 | 2.32 ± 0.37 | 3.22 ± 0.68 | 1.76 ± 0.45 | 2.53 ± 0.56 |
| Measured LAI | 2.14 | | | 2.29 | | | 3.14 | | |
| Difference (%) | 5.6 | -31.31 | 6.07 | 0.13 | -33.62 | 1.31 | 2.55 | -43.95 | 19.43 |

(Table 2). The error of ECOM-LAI compared to measured LAI was 5.6%, 0.1%, and 2.6%, for plots A, B and C, respectively (Table 2). On the other hand, the calculated CI-LAI with 50% threshold was 1.5 ± 0.3 , 1.5 ± 0.4 , and $1.8 \pm 0.5 \text{ m}^2 \text{ m}^{-2}$, and with 75% threshold they were 2.3 ± 0.3 , 2.3 ± 0.4 , and $2.6 \pm 0.6 \text{ m}^2 \text{ m}^{-2}$, for each plot, respectively (Table 2). Therefore, CI-LAI underestimated the measured LAI at the 50% threshold but was comparable with the 75% threshold (except in plot C).

4. Conclusions

This work showed the usefulness of the entropy crossover method (ECOM) to determine the OTV for separating the foreground and background in hemispherical photographs. Together, the ECOM and the gap fraction method were suitable for the calculation of LAI. The robustness of the ECOM in working with different sky luminosity was a desirable characteristic for LAI calculation. The confidence of the calculated LAI from ECOM and the gap fraction methods was demonstrated over two different Brazilian ecosystems including Amazon rainforest and pasture, where the maximum error observed with respect to observations was ~6%. This method also provided and estimate of the clumping factor, an important parameter for ecological and modeling studies.

Our methodology not only provides accurate estimates of LAI, but also is easy to implement, automatic, fast, and reduces the storage size of hemispherical photographs. As such, the calculated LAI values can be obtained in situ immediately after image collection.

Acknowledgements

Many thanks to the LAB-ecology office at Santarém, Pará, Brazil, for letting us use its facilities and equipment from 27 May to 11 June 2001. Thanks to Dr. Jing Ming Chen at the Department of Geography, University of Toronto, who suggested to the first author the use of histogram information to estimate the LAI.

REFERENCES

Anhuf, D., Rollenbeck, R., 2001. Canopy structure of the rio Surumoni rain forest (Venezuela) and its influence on microclimate. *Ecotropica* 7, 21–32.

Asner, G.P., Broadbent, E.N., Oliveira, P.J.C., Keller, M., Knapp, D.E., Silva, J.N.M., 2006. Condition and fate of logged forests in the Brazilian Amazon. *Proceedings of the National Academy of Sciences of the United States of America* 103 (34), 12947–12950.

Campbell, G.S., 1986. Extinction coefficients for radiation in plant canopies calculated using and ellipsoidal inclination angle distribution. *Agricultural and Forest Meteorology* 36, 317–321.

Chen, J.M., Black, T.A., 1992. Foliage area and architecture of plant canopies from sunfleck size distributions. *Agricultural and Forest Meteorology* 60, 249–266.

- Chen, J.M., Cihlar, J., 1995. Plant canopy gap size analysis theory for improving optical measurements of leaf-area index. *Applied Optics* 34, 6211–6222.
- Costa, M.H., Foley, J., 2000. Combined effects of deforestation and doubled atmospheric CO₂ on the climate of Amazonia. *Journal of Climate* 13, 18–34.
- da Rocha, H.R., Goulden, M.L., Miller, S.D., Menton, M.C., Pinto, L.D.V.O., Freitas, H.C., Figueira, A.M.S., 2004. Seasonality of water and heat fluxes over a tropical forest in eastern Amazonia. *Ecological Applications* 14 (4), S22–S32.
- Goulden, M.L., Miller, S.D., da Rocha, H.R., Menton, M.C., Freitas, H.C., Figueira, A.M.S., Sousa, C.A.D., 2004. Diel and seasonal patterns of tropical forest CO₂ exchange. *Ecological Applications* 14 (4), S42–S54.
- Huete, A., Didan, K., Shimabukuro, Y., Ratana, P., Saleska, S., Hutyrá, L., Yang, W., Nemani, R., Myneni, R., 2006. Amazon rainforests green-up with sunlight in the dry season. *Geophysical Research Letters* 33, L06405, doi:10.1029/2005GLO25583.
- Jansing, E., Albert, T., Chenoweth, D., 1999. Two-dimensional entropic segmentation. *Pattern Recognition Letters* 20, 329–336.
- Jonckheere, I., Fleck, S., Nackaerts, K., Muys, B., Coppin, P., Weiss, M., Baret, F., 2004. Review of methods for in situ leaf area index determination. Part I. Theories, sensors and hemispherical photography. *Agricultural and Forest Meteorology* 121, 19–35.
- Jonckheere, I.G., Muys, B., Coppin, P.R., 2005. Derivative analysis for in situ high dynamic range hemispherical photography and its application in forest stands. *IEEE Geoscience and Remote Sensing Letters* 2, 296–300.
- Lang, A.R.G., Xiang, Y., 1986. Estimation of leaf area index from transmission of direct sunlight in discontinuous canopy. *Agricultural and Forest Meteorology* 35, 229–243.
- Leblanc, S.G., Chen, J.M., Fernandes, R., Deering, D.W., Conley, A., 2005. Methodology comparison for canopy structure parameters extraction from digital hemispherical photography in boreal forest. *Agricultural and Forest Meteorology* 129, 187–207.
- Miller, S.D., Goulden, M.L., da Rocha, H.R., 2007. The effect of canopy gaps on subcanopy ventilation and scalar fluxes in a tropical forest. *Agricultural and Forest Meteorology* 142 pp. 25–24.
- Monteith, J.L., Unsworth, M.H., 1990. *Principles of Environmental Physics*, second Edition. Edward Arnold, London, 291 pp.
- Myneni, R.B., Yang, W., Nemani, R.R., Huete, A.R., Dickinson, R.E., Knyazikhin, Y., Didan, K., Fu, R., Negrón Juárez, R.I., Saatchi, S., Hashimoto, H., Ichii, K., Shabanov, N.V., Tan, B., Ratana, P., Privette, J.L., Morisette, J.T., Vermote, E.F., Roy, D.P., Wolfe, R.E., Fried, M.A., Running, S.W., Votava, P., Saleous, N.Z., Devadiga, S., Su, Y., Salomonson, V.V., 2007. Large seasonal swings in leaf area of Amazon rainforest. In: *Proceedings of the National Academy of Sciences of the United States of America*. 104(12), pp. 4820–4823.
- Nilson, T., 1971. A theoretical analysis of the frequency of gaps in plant stands. *Agricultural and Forest Meteorology* 8, 25–38.
- Nobre, C.A., Silva Dias, M.A.F., Culf, A., Polcher, J., Gash, J.H., Marengo, J., Avissar, R., 2004. The Amazonian climate. In: Kabat, P., et al. (Eds.), *Vegetation, Water, Humans and the Climate*. Springer Verlag, New York, pp. 79–92.
- Norman, J.M., Campbell, G.S., 1989. Canopy Structure. In: Pearcy, R.W., Ehlesinger, J., Mooney, H.A., Rundel, P.W. (Eds.), *Plant Physiological Ecology. Field Methods and Instrumentation*. Chapman and Hall, London, pp. 301–325.
- Parton, W.J., Haxeltine, A., Thornton, P., Anne, R., Hartman, 1996. Ecosystem sensitivity to land-surface models and leaf area index. *Global and Planetary Change* 13, 89–98.
- Roberts, J., Cabral, O.M., da Costa, J.P., McWilliam, A., de Sá, T., 1996. An overview of the leaf area index and physiological measurements during ABRACOS. In: Gash, J., Nobre, C., Roberts, J., Victória, R. (Eds.), *Amazon Deforestation and Climate*. J. Wiley & Sons, Chichester, UK, pp. 287–306.
- Sahoo, P.K., Soltani, S., Wong, K.C., 1988. A survey of thresholding techniques. *Computer Vision, Graphics, and Image Processing* 41, 229–232.
- Sahoo, P.K., Slaaf, D.W., Albert, T.A., 1997. Threshold selection using a minimal histogram entropy difference. *Optical Engineering* 36 (7), 1976–1981.
- Sakai, R.K., Fitzjarrald, D.R., Moraes, O.L.L., Staebler, R.M., Acevedo, O.C., Czikowsky, M.J., Silva, R., Brait, E., Miranda, V., 2003. Land-use change effects on local energy, water and carbon balances in an Amazonian agricultural field. *Global Change Biology* 10 (5), 895–907.
- Souza C.A.D., Maia, A.R., Figueira, A.M.S., Suemitsu, C., Goulden, M.L., Miller, S.D., da Rocha, H.R., 2003. Floristic survey and analysis of the phytosociologic structure of one section of the Tapajos National Forest located at Km 83 of the BR-163 highway, Santarem, Para. In: 54th Brazilian Botanical Congress, Para, Brazil. Ref. No. 0965-2. (Portuguese).
- Stenberg, P., 1996. Correcting LAI-2000 for the clumping of needles in shoots of conifers. *Agricultural and Forest Meteorology* 79, 1–8.
- van Gardingen, P.R., Jackson, G.E., Hernandez-Daumas, S., Russell, G., Sharp, L., 1999. Leaf area index estimates obtained for clumped canopies using hemispherical photography. *Agricultural and Forest Meteorology* 94, 243–257.
- Weiss, M., Baret, F., Smith, G., Jonckheere, I., Coppin, P., 2004. Review of methods for in situ leaf area index determination. Part II. Estimation of LAI, errors and sampling. *Agricultural and Forest Meteorology* 121, 37–53.
- Wright, I., Nobre, C.A., Tomasella, J., da Rocha, H.R., Roberts, J., Vertamatti, E., Culf, A., Alvalá, R., Hodnett, M., Ubarana, V., 1996. Towards a GCM surface parameterisation for Amazonia. In: Gash, J., Nobre, C., Roberts, J., Victória, R. (Eds.), *Amazon Deforestation and Climate*. J. Wiley & Sons, Chichester, UK, pp. 473–504.